Quantum walks in synthetic gauge fields with three-dimensional integrated photonics

Octavi Boada,[1] Leonardo Novo,[1,2] Fabio Sciarrino,[3] and Yasser Omar[1,2]

[1]*Instituto de Telecomunicações, Physics of Information and Quantum Technologies Group, 1049-001 Lisbon, Portugal*

[2]*Instituto Superior Técnico, Universidade de Lisboa, 1049-001 Lisbon, Portugal*

[3]*Dipartimento di Fisica, Sapienza Università di Roma, 00185 Roma, Italy*

(Received 31 March 2015; revised manuscript received 2 March 2016; published 23 January 2017)

There is great interest in designing photonic devices capable of disorder-resistant transport and information processing. In this work we propose to exploit three-dimensional integrated photonic circuits in order to realize two-dimensional discrete-time quantum walks in a background synthetic gauge field. The gauge fields are generated by introducing the appropriate phase shifts between waveguides. Polarization-independent phase shifts lead to an Abelian or magnetic field, a case we describe in detail. We find that, in the disordered case, the magnetic field enhances transport due to the presence of topologically protected chiral edge states that do not localize. Polarization-dependent phase shifts lead to effective non-Abelian gauge fields, which could be adopted to realize Rashba-like quantum walks with spin-orbit coupling. Our work introduces a flexible platform for the experimental study of multiparticle quantum walks in the presence of synthetic gauge fields, which paves the way towards topologically robust transport of many-body states of photons.

DOI: 10.1103/PhysRevA.95.013830

I. INTRODUCTION

A long-standing aim in condensed matter physics is to understand the behavior of electrons in two-dimensional systems in the presence of a magnetic field [1]. The reasons for this are both of fundamental and of applied nature. When the system is well described by weakly interacting quasielectrons, it is known that topologically protected edge states akin to those of topological insulators [2] are present. Strongly interacting electrons in a magnetic field arrange themselves in nonstandard states of matter [3] that cannot be described by a local order parameter and the present topological order [4]. The excitations of this state of matter may present non-Abelian statistics, which could be used for topologically protected quantum computation [5].

The promise of ground-breaking applications together with the richness of the underlying physics of two-dimensional (2D) quantum particles in a magnetic field has made these systems a favorite subject of quantum simulator proposals [6]. In these quantum simulators (physical systems unnaturally made to behave according to a specific *model*) the magnetic field is artificial, i.e., synthetic. Instead of using charged particles in an actual magnetic field, in a quantum simulator one typically uses neutral particles upon which the effects of a fictitious magnetic field are imposed. For neutral cold-atom approaches, methods used to generate a synthetic magnetic field include rapid rotation [7,8], Raman-laser-induced Berry phases [9], laser-stimulated tunneling in optical lattices [10–15], or lattice shaking [16].

An alternative approach to quantum simulation is to directly implement the time evolution of the system, as opposed to engineering the underlying Hamiltonian. Quantum walks (QWs) [17] are a prominent example of this idea and have been realized in a variety of platforms, including neutral trapped atoms [18], trapped ions [19,20], and nuclear magnetic resonance in continuous [21] and discrete time [22]. A promising platform is photonic quantum simulators [23], which have been used to simulate QWs in the bulk [24,25] and in waveguide lattices [26], as well as photon time-bin-encoded QWs [27]. Furthermore, two-particle QWs [28] have been realized in integrated photonic circuits using quasiplanar geometries [29–31], nonplanar circuits in a crisscross configuration [32,33], and Anderson localization has been reported in the disordered case [34].

Discrete-time QWs (DTQWs) in one dimension may be implemented with a planar integrated photonic circuit (IPC) forming an array of beam splitters [31]. Each beam splitter performs the coin and step operator at the same time, shifting the photon left and right in quantum superposition. Successive beam splitters create further superpositions, leading to the genuinely quantum interference phenomena that are characteristic of QWs. In this implementation, time is encoded in the direction of propagation of the photon in the IPC.

A promising development in IPC technology is the capability to print the waveguides in a truly 3D configuration. In particular, it is possible to implement quantum walks on a 2D lattice using a 3D network of beam splitters. In such a network, each waveguide corresponds to one lattice site and there are vertical and horizontal beam splitters, which shift the photon wave function in an up-down and left-right superposition, respectively [see Fig. 1(c)]. Similarly to the implementation of 1D quantum walks, the time is encoded in the spatial direction of propagation of the photon.

In this work we propose 3D integrated circuits to realize 2D QWs in a synthetic gauge field. This is accomplished by introducing controlled phase shifts between waveguides at the beam splitters. The phase shifts are chosen in such a way that the photons gain global phases when going around a closed loop, leading to the Aharonov-Bohm effect [35] [see Fig. 1(a)]. Polarization-independent phase shifts lead to an Abelian or magnetic field, while polarization-dependent phase shifts lead to a non-Abelian gauge field [36]. Our scheme may be readily generalized to QWs of two or more photons [28], allowing for the implementation of QW exhibiting topological features [37,38] in the multiphoton case in an IPC. Furthermore, the spatial dependence of the effective gauge field is highly tunable, thus allowing for synthetic gauge fields

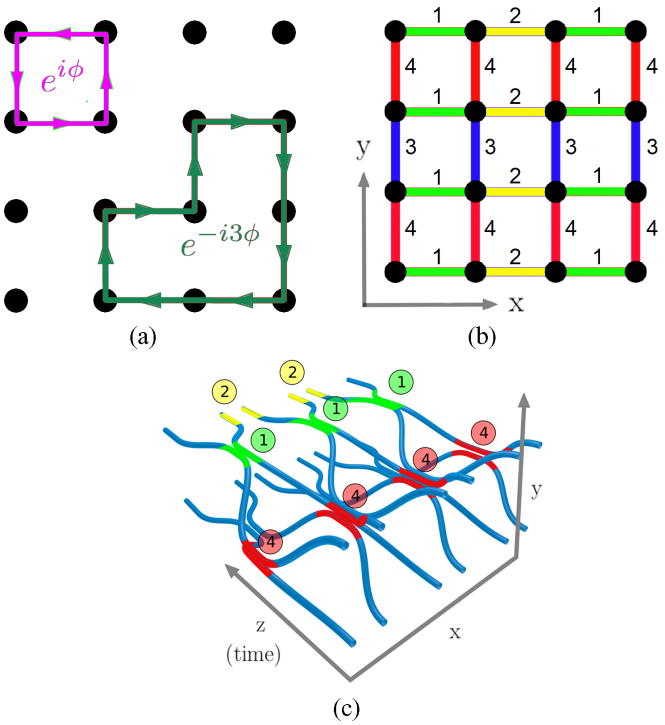

FIG. 1. (a) Accumulated phase acquired by the quantum walker going around two examples of closed trajectories with opposite chirality. This phase depends only on the chirality and the number of elementary cells inside the loop, as in the Aharanov-Bohm effect experienced by a charged particle in a constant magnetic field. (b) In the proposed implementation of the 2D DTQW, the links of the lattice are divided into four groups; each group is depicted with its respective color and number. The motivation is that each site of the lattice corresponds to one waveguide and each link to a beam splitter per time step. Since a beam splitter can only couple two waveguides, the links are divided into four different groups, which together cover the whole lattice. Each group corresponds to a set of commuting beam splitters that implement a unitary U_i from Eq. (5). (c) Diagram of a part of the proposed 3D photonic circuit that realizes the DTQW on a 2D lattice. The z axis represents the direction of time, while the xy plane represents the two spatial dimensions where the QW takes place. One step of the DTQW is composed of four substeps. In each substep, the waveguides are coupled according to the different groups of links depicted in (b). In this scheme, three out of the four different groups of links (beam splitters) from (b) are depicted, with its respective color and number. Each substep implements a set of mutually commuting beam splitters, according to Eq. (5), which can be applied simultaneously. Subsequent substeps could be implemented in the same way along the z direction.

in exotic configurations, such as magnetic monopoles, with no added difficulties. There is great interest in engineering photonic technologies with topologically protected properties [39]. Although several examples of photonic systems with topologically protected edge states have been proposed [40–42] and realized [43,44] with laser light, such as the quantum Hall effect and the Floquet topological insulator [45], our proposal is to realize quantum walks in effective gauge fields in the few-walker regime, using single photons.

II. A 2D QW IN A SYNTHETIC MAGNETIC FIELD WITH AN IPC

The evolution of a charged bosonic particle in a 2D lattice with a perpendicular magnetic field is described by the Hamiltonian

$$H = J \sum_{m,n} (e^{i\phi m} a^{\dagger}_{m,n+1} a_{m,n} + a^{\dagger}_{m+1,n} a_{m,n} + \text{H.c.}). \quad (1)$$

The operators $a^{\dagger}_{m,n}$ and $a_{m,n}$ create and destroy one particle at site (m,n) of the lattice, respectively, and obey bosonic commutation relations. The constant J is an arbitrary energy scale and ϕ is the magnetic flux per plaquette. The key feature of this Hamiltonian is that hopping in one of the directions of the lattice entails the acquisition of a position-dependent phase, breaking time-reversal symmetry. The specific spatial profile of these phases is such that the global phase acquired by a particle going around a closed path on the lattice is position *independent* and equal to $e^{i\phi N}$, where N is the number of elementary cells inside the path [see Fig. 1(a)]. The particular choice of phases is arbitrary [in Eq. (1) we chose the so-called Landau gauge for convenience] as long as the accumulated phase along closed paths leads to the correct global phase. The idea of introducing position-dependent phases has previously been used to realize chiral QWs on graphs [46,47], as well as a QW in an effective electric field [48,49].

Here we use an approach involving coinless discrete-time quantum walks on a 2D lattice where each step implements a position-dependent phase, in analogy with the dynamics given by the Hamiltonian from Eq. (1). We explain how to implement this quantum walk in a 3D IPC and present numerical evidence that its dynamics shows features similar to the one described by (1), namely, the presence of topologically protected edge states. Although in other photonic implementations of discrete-time quantum walks the polarization of the photon is used as the coin [25,27], here we assume the IPC to be polarization independent so that we can use entanglement in the polarization to simulate bosonic and fermionic statistics [28], as previously done in 1D quantum walks in Ref. [34], and so we have a coinless quantum walk. For a general definition and discussion of spreading properties of coinless quantum walks on lattices see Ref. [50].

To implement the quantum walk on the 2D lattice using a 3D IPC, a lattice site in a position (x,y) will correspond to a waveguide engraved in the IPC, also labeled by the position (x,y), which is extended in the z direction, corresponding to the time dimension of the DTQW. The hops of the quantum walk correspond to sequences of beam splitters, which can be implemented by bringing adjacent waveguides close together in such a way that they are evanescently coupled. Each lattice site has at most four neighbors but, since we can only couple two waveguides at a time, it is not possible for the photon in a certain waveguide to hop to all its nearest neighbors in one step. This way, we divide the DTQW into four substeps, as depicted in Fig. 1(b), where the links in green correspond to hopping terms that will be implemented by a unitary matrix U_1, the ones in yellow by U_2, the ones in red by U_3, and finally the ones in blue by U_4. This way, one full step of the quantum

walk will be given by

$$U_{\text{step}} = U_4 U_3 U_2 U_1. \tag{2}$$

This sequence of unitaries can be applied many times along the z direction of the IPC to implement subsequent steps of the quantum walk. A schematic representation of part of the 3D photonic circuit implementing the red, green, and yellow links is shown in Fig. 1(c).

In order to mimic the effect of a magnetic field, we need to construct U_{step} in such a way that if the walker makes a closed path around N elementary cells, it acquires a position-independent phase $e^{i\phi N}$. To show the form of the unitaries U_i that satisfy this requirement, we define the states of the Hilbert space $|x\rangle|y\rangle$, with $x \in \{1, M\}$ and $y \in \{1, M\}$, and say that the photon is in state $|x\rangle|y\rangle$ if it is in the waveguide labeled by the coordinates (x, y). In this basis, we define the hopping operators in the x and y directions as

$$\begin{aligned} V_x = &\frac{1}{\sqrt{2}}(|x\rangle\langle x| + |x+1\rangle\langle x+1|) \\ &+ \frac{i}{\sqrt{2}}(|x\rangle\langle x+1| + |x+1\rangle\langle x|), \end{aligned} \tag{3}$$

$$\begin{aligned} V_y(\phi) = &\frac{1}{\sqrt{2}}(|y\rangle\langle y| + |y+1\rangle\langle y+1|) \\ &+ \frac{i}{\sqrt{2}}(e^{-i\phi}|y\rangle\langle y+1| + e^{i\phi}|y+1\rangle\langle y|), \end{aligned} \tag{4}$$

which corresponds to an unbiased beam-splitter matrix and to a phase-shifted beam splitter, respectively. The operators U_1, U_2, U_3, and U_4 are then defined as

$$\begin{aligned} U_1 &= \sum_{x=0}^{M/2-1} V_{2x+1} \otimes \mathcal{I}_y, \\ U_2 &= \sum_{x=1}^{M/2-1} V_{2x} \otimes \mathcal{I}_y, \\ U_3 &= \sum_{x=1}^{M} \sum_{y=0}^{M/2-1} |x\rangle\langle x| \otimes V_{2y+1}(x\phi), \\ U_4 &= \sum_{x=1}^{M} \sum_{y=1}^{M/2-1} |x\rangle\langle x| \otimes V_{2y}(x\phi). \end{aligned} \tag{5}$$

Here U_3 and U_4 cause the hopping of the photon in the y direction and apply a phase that is proportional to the coordinate x. It can be seen that this quantum walk is chiral in the sense that it breaks time-reversal symmetry (for a discussion of chiral quantum walks see Ref. [47]). Previous experiments have shown full phase-shift controllability between two waveguides, by deforming one of the waveguides and thus creating a difference in the optical path length [34]. Hence, the experimental implementation of U_{step}, although challenging, is within reach of current technology.

The previous construction of beam-splitter matrices mimics the propagation of 2D charged particles in a magnetic field. This is the case because the beam splitters are not translationally invariant and their position dependence is chosen such that a photon going around a closed loop of adjacent waveguides acquires a position-independent phase $e^{i\phi}$ as in the case of the Hamiltonian in Eq. (1). Indeed, we have checked this correspondence numerically, as can be seen in Appendix A, where we compute the spectrum of an effective Hamiltonian $H_{\text{eff}} = i(\Delta T)^{-1} \log_e U_{\text{step}}$, yielding the well-known Hofstadter butterfly [51], a complex self-similar structure that arises in the case of electrons propagating on a 2D lattice in a strong magnetic field. We use units in which the time step ΔT and $\hbar$ are 1.

This relation, however, can be made more precise by looking at the exponential of the magnetic Hamiltonian and performing a Suzuki-Trotter decomposition [see [52] for the decomposition applied to a tight-binding Hamiltonian like that in Eq. (1)]. The key observation to make the connection, which is beyond the scope of this work, is

$$\frac{1}{\sqrt{2}}\begin{pmatrix} 1 & ie^{im\phi} \\ ie^{-im\phi} & 1 \end{pmatrix} = \exp\left[i\frac{\pi}{4}\begin{pmatrix} 0 & e^{im\phi} \\ e^{-im\phi} & 0 \end{pmatrix}\right]. \tag{6}$$

The left-hand side can be viewed as a beam splitter with a phase difference, such as operators $V_y(\phi)$ in Eq. (5), and the right-hand side is the exponential of a hopping term $e^{i\phi m} a^\dagger_{m,n+1} a_{m,n} + e^{-i\phi m} a_{m,n+1} a^\dagger_{m,n}$.

III. SIGNATURES OF THE MAGNETIC FIELD FOR SINGLE PHOTONS

To confirm qualitatively the correspondence between the proposed IPC and the time evolution generated by Eq. (1), we have computed the spectrum of the effective Hamiltonian $H_{\text{eff}} = i \log_e U_{\text{step}}$, where U_{step} is the unitary operator implemented by the proposed optical circuit. In Appendix A we plot the spectrum of H_{eff} as a function of ϕ. We obtain a figure very similar to Hofstadter's butterfly [51].

Furthermore, we investigate the effect of the synthetic magnetic field on the spreading and transport properties of the QW at the single-photon level, with and without disorder. Controlled disorder may be implemented via small random differences in waveguide lengths at the evanescent couplings [34], which lead to fluctuations in each waveguide's optical path (see Appendix B). These fluctuations are static, in the sense that they are not time dependent [z dependent in Fig. 1(c)].

To determine how quickly the QW spreads without disorder, in Fig. 2(a) we plot the variance of the single-particle probability distribution σ^2 as a function of the number of steps, for different values of ϕ, the magnetic flux per plaquette. We identify the position of the particle by the label of the waveguide in which the particle is. This way, the position here is a dimensionless quantity and so is the variance. The initial wave function is localized at the center of the lattice. Although we plot here the result for three values of ϕ, we have observed that the variance is always smaller for $\phi \neq 0$ than for $\phi = 0$. Hence, without disorder the magnetic field is detrimental to the expansion of an initially localized photon wave function. We also study the QW evolution by computing the transport efficiency between two far-apart waveguides in the presence of disorder. We choose one corner of the lattice as an initial site or waveguide and the site at the opposite corner as the target. We introduce absorption at the target waveguide, corresponding to position (M, M), at each step of the QW by replacing the operator U_{step} by $U_{\text{step}}(\mathcal{I} - |M\rangle|M\rangle\langle M|\langle M|)$. Our measure

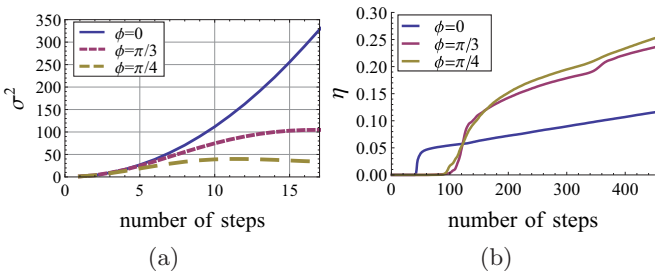

FIG. 2. In an ordered lattice, a magnetic field hinders the spreading of the wave function and quantum transport; in a disordered lattice, a magnetic field enhances transport due to the presence of nonlocalized edge states. (a) Variance of the single-photon wave function vs the number of time steps for different values of the magnetic flux ϕ. The initial state is localized at the center of the lattice. For nonzero ϕ the QW spreads at a slower rate. (b) Transport efficiency η as a function of time in the presence of Gaussian disorder with strength $\delta = 0.1$ (defined in Appendix B). The quantity η measures the accumulated norm at the opposite corner, or the efficiency of quantum transport across the lattice. In the presence of disorder, the applied magnetic field qualitatively enhances transport.

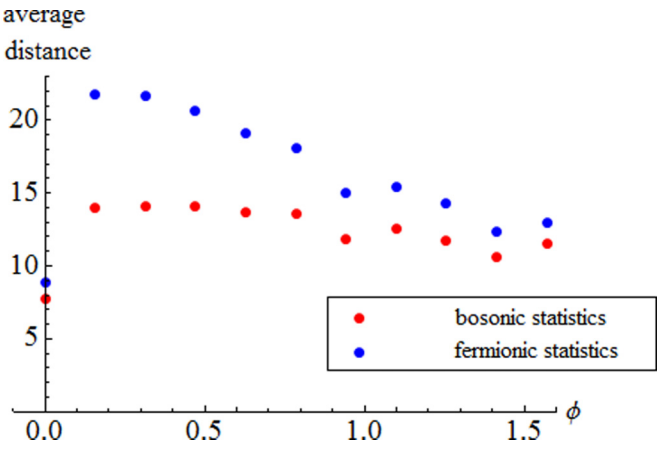

FIG. 3. Average distance between photons for the two-photon quantum walk on the IPC, after 20 steps, in a lattice of size 30×30, for different values of the magnetic flux ϕ. The initial state is localized at positions $(1,1)$ and $(2,1)$ of the lattice and the photons' polarization states are entangled in a symmetric (antisymmetric) way so that the exchange statistics of the wave function is bosonic (fermionic). We observe, as expected, that for bosonic statistics the photons tend to remain closer than in the fermionic case. Also, the presence of the magnetic field greatly increases the distance between the photons, as each particle overcomes Anderson localization due to the nonzero magnetic field.

of transport efficiency η is the accumulated probability of finding the photon at the target state $|\mathcal{T}\rangle = |M\rangle|M\rangle$, $\eta = \sum_t |\langle\mathcal{T}|\psi(t)\rangle|^2$, an approach similar to that used in [53]. Let us stress that η could be measured in an experiment by coupling the target waveguide to a long chain of waveguides as proposed in [33] or to a detector at every time step.

With disorder, low transport efficiency is expected, due to Anderson localization. Interestingly, we find that while in the ordered case a magnetic field slows down the expansion of the QW, in the case of disorder it does the opposite, thus enhancing quantum transport [see Fig. 2(b)]. This is attributable to the presence of chiral edge states (see Fig. 3), which are topologically protected against localization.

IV. A TWO-PHOTON QW WITH A MAGNETIC FIELD

The single-particle probabilities obtained by using one photon as the input state of the IPC can be reproduced by using a classical laser light source. However, if two or more indistinguishable photons are used as input, the probability distribution measured at the output of the circuit has no classical analog and for many photons is, in general, hard to calculate [54,55]. Also, by choosing appropriate entangled states of two photons, the statistics of bosons and fermions can be mimicked [28] and bunching and antibunching phenomena have been observed in 1D QWs [34]. The initial states $|\Psi_0^{\pm}\rangle$ we chose are

$$|\Psi_0^{\pm}\rangle = \frac{1}{\sqrt{2}}[|(1,1);(2,1)\rangle \pm |(2,1);(1,1)\rangle], \qquad (7)$$

where $|(1,1);(2,1)\rangle$ is a two-photon state with one photon in position $(1,1)$ and the other photon in position $(2,1)$. Here we have computed observables for the DTQWs of two entangled photons in a synthetic magnetic field. The average distance between photons is plotted in Fig. 3 for two entangled photons starting at the corner of the lattice. The effect of the particle statistics in this quantity is clear since bosons remain closer than fermions. Also, the presence of the magnetic field increases the average distance between particles, as each particle is able to undergo a QW that is not localized due to disorder, which is a single-particle effect. The presence of two-particle edge states can be seen from the probability that both photons are at the edge of the lattice shown in Appendix C.

V. A NON-ABELIAN 2D QW

Our proposed scheme to realize a magnetic QW with an IPC may be generalized to a non-Abelian magnetic QW, provided the relative phases between adjacent waveguides are made polarization dependent in a controlled way. When polarization is taken into account, a general term coupling two adjacent lattice sites i and j can be written in the form $\sum_{\xi\tau} a_{i\xi}^{\dagger} U_{ij}^{\xi\tau} a_{j\tau} +$ H.c., where ξ and τ run over photon polarizations and now $a_{i\xi}^{\dagger}$ creates a photon at site i with polarization ξ.

Thus, to realize a QW in a non-Abelian synthetic gauge field, the beam-splitter matrices must be polarization dependent, which are now described by 4×4 matrices instead of 2×2. In general, the beam-splitter matrices corresponding to different links of the lattice will not commute with each other and will lead to nontrivial non-Abelian fluxes when the photons go around a closed loop [see Fig. 1(a)]. This is tantamount to a modified Aharonov-Bohm effect, where the photon wave function is multiplied by the Wilson loop [56] instead of a phase.

Remarkably, interesting non-Abelian QWs may be implemented using relatively simple IPCs. In particular, a QW with Rashba spin-orbit coupling [57] may be realized with the choice $U_x = \exp(i\alpha\sigma_y)$ and $U_y = \exp(-i\alpha\sigma_x)$, where σ_x and σ_y are Pauli matrices. In the 3D IPC architecture, this means

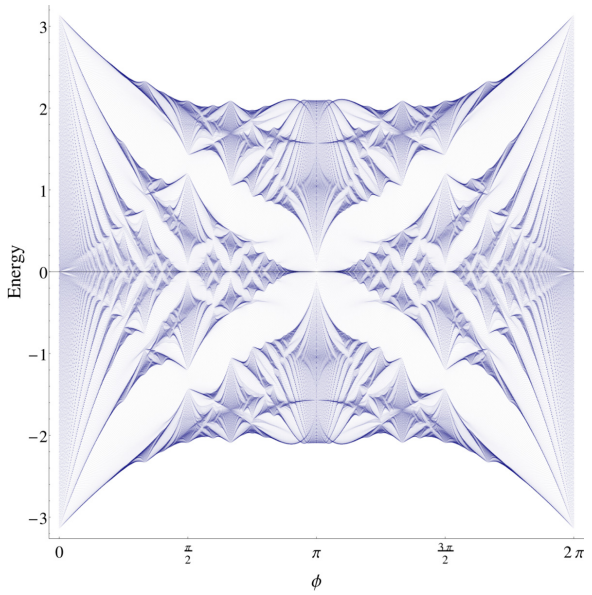

FIG. 4. Spectrum of the effective Hamiltonian $H_{\text{eff}} = i \log_e U_{\text{step}}$ that generates the Abelian QW proposed here, as a function of the magnetic flux per plaquette ϕ. We use units in which the time step ΔT and $\hbar$ are 1.

adjacent waveguides in the x direction are coupled with U_x and those in the y direction with U_y. Note that this choice does not require position-dependent delays between waveguides as the Abelian magnetic field case does. In this scenario, since the circuit is now polarization dependent, it would not be possible to simulate different particle statistics by entangling photons in polarization.

VI. CONCLUSION

We have introduced a scheme that allows implementing quantum walks in synthetic gauge fields using integrated photonic circuits. This scheme requires a strong experimental and technological effort: We need the capability to engineer 3D structures with a significant number of steps. In the past year several improvements have been achieved: an eight-mode fast Fourier transform with 3D structure [58], a reconfigurable phase [59], and operation at telecom wavelength that ensures lower losses and hence the possibility to realize longer chips [59]. Our proposal is well suited for the study of topological insulators at the single- and few-photon levels and it is highly flexible, allowing for the simulation of both Abelian and non-Abelian gauge fields. We have studied the single-photon quantum walk in a constant Abelian or magnetic field and computed experimentally accessible observables, demonstrating topological properties, namely, the presence of edge states enhancing transport across disordered lattices. We have also computed observables for two-particle quantum walks that demonstrate the role of entanglement and magnetic field in the behavior of the walk. Overall, we have shown that the development of 3D integrated photonics can lead to the experimental study of interesting 2D quantum physics with topological features in the few-body regime.

ACKNOWLEDGMENTS

O.B., L.N., and Y.O. are grateful for support from Fundação para a Ciência e a Tecnologia (Portugal) through programs PTDC, POPH, and POCH and projects UID/EEA/50008/2013, IT/QuSim, IT/QuNet, and ProQuNet, partially funded by EU FEDER, and from the EU FP7 project PAPETS (No. GA 323901). Furthermore L.N. acknowledges support from the DP-PMI and FCT (Portugal) through Scholarship No. SFRH/BD/52241/2013. F.S. acknowledges support from the ERC Starting Grant 3D-QUEST (3D Quantum Integrated Optical Simulation; Grant Agreement No. 307783).

APPENDIX A: SPECTRUM OF THE UNITARY IMPLEMENTED BY THE INTEGRATED PHOTONIC CIRCUIT

We have constructed a unitary matrix that implements one time step of the DTQW with a synthetic magnetic field, defined by Eq. (2). This matrix, denoted by U_{step}, can be decomposed in a product of beam splitter and phase shifter matrices, which can be implemented in an IPC. In Fig. 4 we plot the spectrum of the effective Hamiltonian $H_{\text{eff}} = i \log_e U_{\text{step}}$ as a function of ϕ. As expected, we obtain a figure very similar

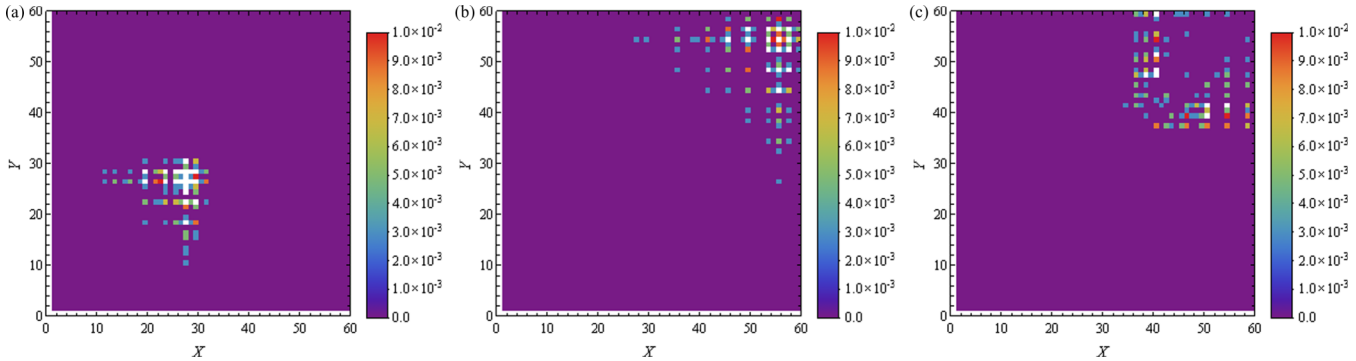

FIG. 5. Simulation of the IPC implementation of a DTQW in a 2D lattice in zero magnetic field without disorder, starting at position $(X,Y) = (1,1)$. The probability distribution of a discrete-time QW on a 60×60 ordered lattice is shown after (a) 20, (b) 40, and (c) 60 time steps. The quantum walk propagates quickly from one corner of the lattice to the opposite corner. The white color corresponds to probabilities above 0.01, which can go up to 0.11 in (a), 0.056 in (b), and 0.016 in (c). The total probability for each plot is (a) 1, (b) 1, and (c) 0.77. The coordinates X and Y are merely waveguide labels, so we do not consider units of distance here.

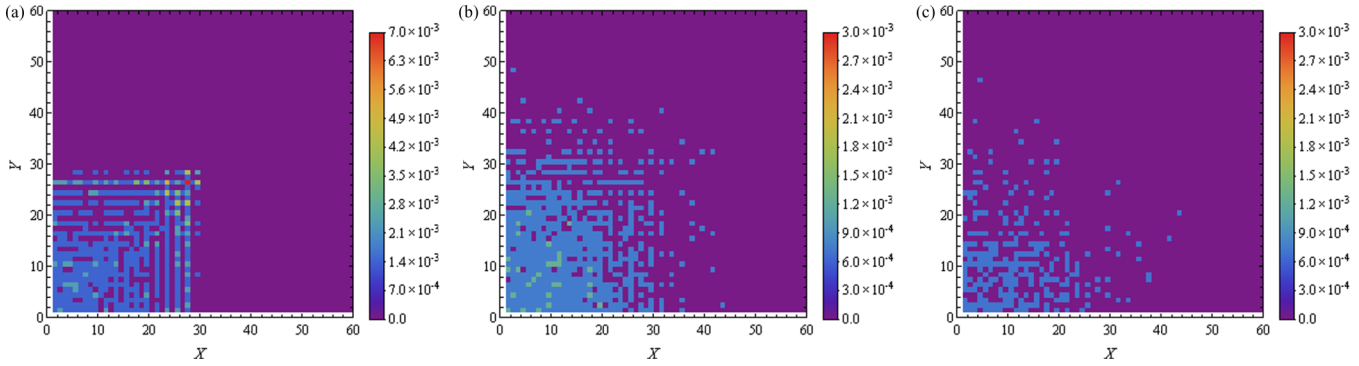

FIG. 6. Simulation of the IPC implementation of a DTQW in a 2D lattice in zero magnetic field with disorder, starting at position $(X,Y) = (1,1)$. The probability distribution of a discrete-time QW on a 60×60 disordered lattice is shown after (a) 20, (b) 40, and (c) 60 steps. The strength of disorder is $\delta = 0.2$ and the magnetic field is set to zero. The presence of disorder hinders the propagation on the lattice and the photon remains localized close to its starting position, resulting in a low transport efficiency to the opposite corner. The probability amplitude is averaged over 20 disorder realizations. Note that the scales of the plots are different, for better visualization. The total probability for each plot is (a) 1, (b) 1, and (c) 0.997. The coordinates X and Y are merely waveguide labels, so we do not consider units of distance here.

to Hofstadter's butterfly [51]. For relatively large lattices (30×30), the spectrum of H_{eff} presents a fractal nature and a structure of gaps that is very reminiscent of Hofstadter's butterfly.

APPENDIX B: TIME EVOLUTION OF SINGLE-PARTICLE QUANTUM WALKS IN A MAGNETIC FIELD

We study the effect of a synthetic Abelian gauge field on the transport properties of a discrete-time 2D QW in the presence of disorder. All simulations have been done with the beam-splitter matrices given in Eqs. (4) and (5). The initial wave function is localized at the lower left corner of the lattice. In Fig. 5 we plot the evolution of the QW without magnetic field and without disorder. There is efficient transport from one corner of the lattice to the other. In Fig. 6 localization close to the initial position is observed for zero magnetic field and disorder; transport from one corner of the lattice to the other is highly inefficient in this case. In Fig. 7 we plot the evolution of the QW for nonzero magnetic field, $\phi = \frac{\pi}{5}$, and in the presence of disorder. Transport from one corner of the lattice to the opposite one is clearly accomplished by edge states, which do not penetrate significantly into the bulk of the lattice.

At each step of the QW, the probability at the target waveguide is subtracted from the wave function, as we introduce absorption by replacing the operator U with $U \exp(-a^{\dagger}_{\text{target}} a_{\text{target}})$. Thus, the deviation from unity of the total probability is equal to the transport efficiency $\eta = \sum_t |\langle \mathcal{T} | \psi(t) \rangle|^2$.

The introduction of static disorder in the DTQW in a 2D lattice is done by multiplying each beam-splitter matrix V_x or $V_y(\phi)$, defined in Eqs. (3) and (4), by a matrix with random phases in the diagonal,

$$V^{\text{dis}}_{x,y} = \begin{pmatrix} e^{i\epsilon_i} & 0 \\ 0 & e^{i\epsilon_j} \end{pmatrix} V_{x,y}. \tag{B1}$$

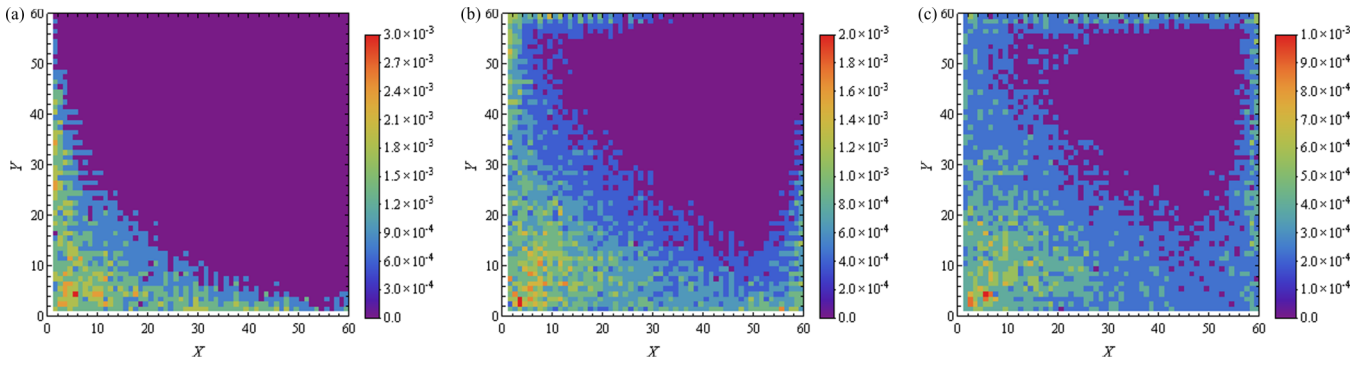

FIG. 7. Simulation of the IPC implementation of a DTQW in a 2D lattice in nonzero magnetic field with disorder, starting at position $(X,Y) = (1,1)$. The probability distribution of a discrete-time QW on a 60×60 disordered lattice with magnetic field is shown after (a) 50, (b) 100, and (c) 150 steps. The strength of disorder is $\delta = 0.2$ and the magnetic field is $\phi = \pi/5$. The quantum walk propagates mainly along the edges of the lattice. The presence of topologically protected edge states that do not localize allows for the propagation of the photon to the opposite corner of the lattice. Here we investigate a larger number of steps as compared to Figs. 5 and 6, in order to see the propagation to the opposite corner of the lattice $(X,Y) = (60,60)$. The probability amplitude is averaged over 20 disorder realizations. Note that the scales of the plots are different, for better visualization. The total probability for each plot is (a) 1, (b) 1, and (c) 0.984. The coordinates X and Y are merely waveguide labels, so we do not consider units of distance here.

The quantities ϵ_i are sampled from a normal distribution with standard deviation δ, which we will refer to as the disorder strength. This will lead to a unitary U'_{step} defining the step of the quantum walk with static disorder. Note that time-dependent disorder, i.e., if U'_{step} depends on the step number, would lead to dephasing of the QW [34].

APPENDIX C: EVIDENCE OF TWO-PHOTON EDGE STATES

A quantity that can easily be calculated from the probability distribution of the position of the photons at the output of the IPC is the probability that the photons leave the circuit in a waveguide that belongs to the edge of the 2D lattice. For the two-photon quantum walk, we calculate this probability for a lattice of size 30×30, after 20 steps, and for variable magnetic flux ϕ (see Fig. 8). The two photons are inserted in the circuit in the corner of the lattice at the position $(X,Y) = (1,1)$ and its nearest neighbor in the x direction at the position $(2,1)$. The two photons are entangled in polarization in a symmetric (antisymmetric) way in order to simulate bosonic (fermionic) statistics [28,34]. We see that, for zero magnetic field, it is very unlikely that the photons leave the circuit by the edge of the lattice, but with magnetic field this probability increases up to $\approx 15\%$. It is interesting that the particle statistics does not affect much this probability, unlike what happens with the average distance between particles shown in the main text.

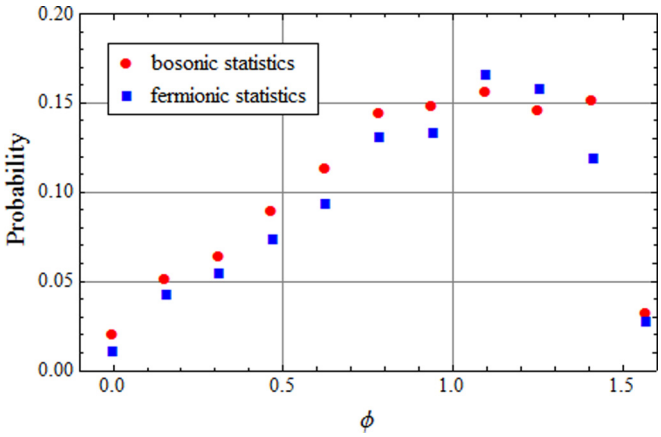

FIG. 8. Probability that the two photons are at the edge of the lattice for the quantum walk on the IPC, after 20 steps, in a lattice of size 30×30, for different values of the magnetic flux ϕ. If the photons' polarization states are entangled in a symmetric (antisymmetric) way, their statistics is bosonic (fermionic). The presence of the magnetic field increases significantly the probability that the two photons are at the edge. However, the exchange statistics of the two-photon wave function does not affect this quantity much.

[1] K. v. Klitzing, G. Dorda, and M. Pepper, Phys. Rev. Lett. **45**, 494 (1980).
[2] M. Z. Hasan and C. L. Kane, Rev. Mod. Phys. **82**, 3045 (2010).
[3] R. B. Laughlin, Phys. Rev. Lett. **50**, 1395 (1983).
[4] X.-G. Wen and Q. Niu, Phys. Rev. B **41**, 9377 (1990).
[5] C. Nayak, S. H. Simon, A. Stern, M. Freedman, and S. D. Sarma, Rev. Mod. Phys. **80**, 1083 (2008).
[6] I. Buluta and F. Nori, Science **326**, 108 (2009).
[7] K. W. Madison, F. Chevy, W. Wohlleben, and J. Dalibard, Phys. Rev. Lett. **84**, 806 (2000).
[8] J. Abo-Shaeer, C. Raman, J. Vogels, and W. Ketterle, Science **292**, 476 (2001).
[9] J. Dalibard, F. Gerbier, G. Juzeliūnas, and P. Öhberg, Rev. Mod. Phys. **83**, 1523 (2011).
[10] D. Jaksch and P. Zoller, New J. Phys. **5**, 56 (2003).
[11] F. Gerbier and J. Dalibard, New J. Phys. **12**, 033007 (2010).
[12] A. Celi, P. Massignan, J. Ruseckas, N. Goldman, I. B. Spielman, G. Juzeliūnas, and M. Lewenstein, Phys. Rev. Lett. **112**, 043001 (2014).
[13] Y.-J. Lin, R. L. Compton, K. Jimenez-Garcia, J. V. Porto, and I. B. Spielman, Nature (London) **462**, 628 (2009).
[14] H. Miyake, G. A. Siviloglou, C. J. Kennedy, W. C. Burton, and W. Ketterle, Phys. Rev. Lett. **111**, 185302 (2013).
[15] M. Aidelsburger, M. Atala, M. Lohse, J. T. Barreiro, B. Paredes, and I. Bloch, Phys. Rev. Lett. **111**, 185301 (2013).
[16] J. Struck, C. Ölschläger, R. Le Targat, P. Soltan-Panahi, A. Eckardt, M. Lewenstein, P. Windpassinger, and K. Sengstock, Science **333**, 996 (2011).
[17] J. Kempe, Contemp. Phys. **44**, 307 (2003).
[18] M. Karski, L. Förster, J.-M. Choi, A. Steffen, W. Alt, D. Meschede, and A. Widera, Science **325**, 174 (2009).
[19] H. Schmitz, R. Matjeschk, C. Schneider, J. Glueckert, M. Enderlein, T. Huber, and T. Schaetz, Phys. Rev. Lett. **103**, 090504 (2009).
[20] F. Zähringer, G. Kirchmair, R. Gerritsma, E. Solano, R. Blatt, and C. F. Roos, Phys. Rev. Lett. **104**, 100503 (2010).
[21] J. Du, H. Li, X. Xu, M. Shi, J. Wu, X. Zhou, and R. Han, Phys. Rev. A **67**, 042316 (2003).
[22] C. A. Ryan, M. Laforest, J. C. Boileau, and R. Laflamme, Phys. Rev. A **72**, 062317 (2005).
[23] A. Aspuru-Guzik and P. Walther, Nat. Phys. **8**, 285 (2012).
[24] P. Zhang, X.-F. Ren, X.-B. Zou, B.-H. Liu, Y.-F. Huang, and G.-C. Guo, Phys. Rev. A **75**, 052310 (2007).
[25] M. A. Broome, A. Fedrizzi, B. P. Lanyon, I. Kassal, A. Aspuru-Guzik, and A. G. White, Phys. Rev. Lett. **104**, 153602 (2010).
[26] H. B. Perets, Y. Lahini, F. Pozzi, M. Sorel, R. Morandotti, and Y. Silberberg, Phys. Rev. Lett. **100**, 170506 (2008).
[27] A. Schreiber, K. N. Cassemiro, V. Potoček, A. Gábris, P. J. Mosley, E. Andersson, I. Jex, and C. Silberhorn, Phys. Rev. Lett. **104**, 050502 (2010).
[28] Y. Omar, N. Paunković, L. Sheridan, and S. Bose, Phys. Rev. A **74**, 042304 (2006).
[29] A. Peruzzo, M. Lobino, J. C. Matthews, N. Matsuda, A. Politi, K. Poulios, X.-Q. Zhou, Y. Lahini, N. Ismail, K. Wörhoff *et al.*, Science **329**, 1500 (2010).
[30] J. O. Owens, M. A. Broome, D. N. Biggerstaff, M. E. Goggin, A. Fedrizzi, T. Linjordet, M. Ams, G. D. Marshall, J. Twamley, M. J. Withford *et al.*, New J. Phys. **13**, 075003 (2011).
[31] L. Sansoni, F. Sciarrino, G. Vallone, P. Mataloni, A. Crespi, R. Ramponi, and R. Osellame, Phys. Rev. Lett. **108**, 010502 (2012).

[32] K. Poulios, R. Keil, D. Fry, J. D. Meinecke, J. C. Matthews, A. Politi, M. Lobino, M. Gräfe, M. Heinrich, S. Nolte *et al.*, Phys. Rev. Lett. **112**, 143604 (2014).
[33] A. Crespi, L. Sansoni, G. Della Valle, A. Ciamei, R. Ramponi, F. Sciarrino, P. Mataloni, S. Longhi, and R. Osellame, Phys. Rev. Lett. **114**, 090201 (2015).
[34] A. Crespi, R. Osellame, R. Ramponi, V. Giovannetti, R. Fazio, L. Sansoni, F. De Nicola, F. Sciarrino, and P. Mataloni, Nat. Photon. **7**, 322 (2013).
[35] Y. Aharonov and D. Bohm, Phys. Rev. **115**, 485 (1959).
[36] J. B. Kogut, Rev. Mod. Phys. **51**, 659 (1979).
[37] T. Kitagawa, M. S. Rudner, E. Berg, and E. Demler, Phys. Rev. A **82**, 033429 (2010).
[38] T. Kitagawa, M. A. Broome, A. Fedrizzi, M. S. Rudner, E. Berg, I. Kassal, A. Aspuru-Guzik, E. Demler, and A. G. White, Nat. Commun. **3**, 882 (2012).
[39] A. B. Khanikaev, S. H. Mousavi, W.-K. Tse, M. Kargarian, A. H. MacDonald, and G. Shvets, Nat. Mater. **12**, 233 (2013).
[40] F. D. M. Haldane and S. Raghu, Phys. Rev. Lett. **100**, 013904 (2008).
[41] K. Fang, Z. Yu, and S. Fan, Nat. Photon. **6**, 782 (2012).
[42] M. Schmidt, S. Keßler, V. Peano, O. Painter, and F. Marquardt, Optica **2**, 635 (2015).
[43] M. Hafezi, E. A. Demler, M. D. Lukin, and J. M. Taylor, Nat. Phys. **7**, 907 (2011).
[44] S. Mittal, J. Fan, S. Faez, A. Migdall, J. M. Taylor, and M. Hafezi, Phys. Rev. Lett. **113**, 087403 (2014).
[45] M. C. Rechtsman, J. M. Zeuner, Y. Plotnik, Y. Lumer, D. Podolsky, F. Dreisow, S. Nolte, M. Segev, and A. Szameit, Nature (London) **496**, 196 (2013).
[46] Z. Zimboras, M. Faccin, Z. Kadar, J. D. Whitfield, B. P. Lanyon, and J. Biamonte, Sci. Rep. **3**, 2361 (2013).
[47] D. Lu, J. D. Biamonte, J. Li, H. Li, T. H. Johnson, V. Bergholm, M. Faccin, Z. Zimborás, R. Laflamme, J. Baugh *et al.*, Phys. Rev. A **93**, 042302 (2016).
[48] C. Cedzich, T. Rybár, A. H. Werner, A. Alberti, M. Genske, and R. F. Werner, Phys. Rev. Lett. **111**, 160601 (2013).
[49] M. Genske, W. Alt, A. Steffen, A. H. Werner, R. F. Werner, D. Meschede, and A. Alberti, Phys. Rev. Lett. **110**, 190601 (2013).
[50] R. A. M. Santos, R. Portugal, and S. Boettcher, Quant. Inf. Process. **14**, 3179 (2015).
[51] D. R. Hofstadter, Phys. Rev. B **14**, 2239 (1976).
[52] G. G. Batrouni and R. T. Scalettar, Phys. Rev. B **46**, 9051 (1992).
[53] J. K. Asboth and J. M. Edge, Phys. Rev. A **91**, 022324 (2015).
[54] S. Aaronson and A. Arkhipov, in *Proceedings of the 43rd Annual ACM Symposium on Theory of Computing* (ACM, New York, 2011), pp. 333–342.
[55] A. Crespi, R. Osellame, R. Ramponi, D. J. Brod, E. F. Galvão, N. Spagnolo, C. Vitelli, E. Maiorino, P. Mataloni, and F. Sciarrino, Nat. Photon. **7**, 545 (2013).
[56] M. E. Peskin and D. V. Schroeder, *An Introduction to Quantum Field Theory* (Westview, Boulder, 1995).
[57] E. Rashba, Sov. Phys. Solid State **2**, 1109 (1960).
[58] A. Crespi, R. Osellame, R. Ramponi, M. Bentivegna, F. Flamini, N. Spagnolo, N. Viggianiello, L. Innocenti, P. Mataloni, and F. Sciarrino, Nat. Commun. **7**, 10469 (2016).
[59] F. Flamini, L. Magrini, A. S. Rab, N. Spagnolo, V. D'Ambrosio, P. Mataloni, F. Sciarrino, T. Zandrini, A. Crespi, R. Ramponi, and R. Osellame, Light: Science and Applications **4**, e354 (2015).